

Kondo Effect in a Quantum-Dot-Topological-Superconductor Junction

Minchul Lee,¹ Jong Soo Lim,² Heunghwan Khim,³ and Rosa López^{2,4}

¹Department of Applied Physics, College of Applied Science, Kyung Hee University, Yongin 446-701, Korea

²Institut de Física Interdisciplinària i de Sistemes Complexos IFISC (CSIC-UIB), E-07122 Palma de Mallorca, Spain

³Department of Physics, Korea University, Seoul 136-701, Korea

⁴Departament de Física, Universitat de les Illes Balears, E-07122 Palma de Mallorca, Spain

(Dated: March 4, 2022)

We investigate the dynamical and transport features of a Kondo dot side-coupled to a topological superconductor (TS). The Majorana fermion states (MFS) formed at the ends of the TS are found to be able to alter the Kondo physics profoundly: For the ideal setup where the MFS do not overlap ($\epsilon_m = 0$) a finite dot-MFS coupling (Γ_m) reduces the unitary-limit value of the linear conductance by exactly a factor 3/4 in the Kondo-dominant regime ($\Gamma_m < T_K$), where T_K is the Kondo temperature. In the Majorana-fermion dominant phase ($\Gamma_m > T_K$), on the other hand, the spin-split Kondo resonance takes place due to the MFS-induced Zeeman splitting, which is a genuine many-body effect of the strong Coulomb interaction and the topological superconductivity. We find that the original Kondo resonance is fully restored once the MFSs are strongly hybridized ($\epsilon_m > \Gamma_m$). This unusual interaction between the Kondo effect and the MFS can thus serve to detect the Majorana fermions unambiguously and quantify the degree of overlap between the MFSs in the TS.

PACS numbers: 73.63.-b, 73.50.Fq, 73.63.Kv

Introduction.— One of the most paradigmatic effects in condensed matter physics is the celebrated *Kondo effect*. The ground state of a metal that contains magnetic impurities consists of a many-body singlet state where the localized impurities are entangled with the conducting states [1]. The Kondo effect has been observed in manufactured nanostructures such as quantum dots (QDs) [2–7], carbon nanotubes [8–10], nanowires [11], and so on. The great advantage of the observation of the Kondo effect in artificial set-ups is its high tunability and control by means of the application of electrical gates or external fields (e.g., magnetic field, an ac signal) that drives the Kondo state towards nonequilibrium situations [12–15]. Nevertheless, the Kondo physics can be modified not only externally but also intrinsically by utilizing different type of contacts materials, say, superconducting or ferromagnetic ones [16–21].

Since the discovery of the topological materials [22, 23] there has been a large number of proposals for the physical realization of low-energy quasiparticle excitations behaving as Majorana fermions [24–27]. Recently, Mourik *et al.* [28] reported the detection of such quasiparticles in InSb nanowires brought into proximity with a *s*-wave superconductor in the presence of both magnetic field and spin-orbit interaction [29–31]. Later on, other groups have also showed signatures of Majorana physics in similar set-ups [32–34]. Therefore, it is quite natural to think about more intricate scenarios by combining Kondo-like artificial impurities with localized Majorana fermions hosted in topological materials.

The purpose of this work is to analyze a prototypical system to probe the interplay between Kondo and Majorana physics by means of usual transport measurements. The system consists of a quantum dot attached to two normal contacts, in which the Kondo correlations can be developed [35–37], and a topological superconductor (TS) [38–41] whose one end is connected to the QD by a tunneling junction. The TS is float-

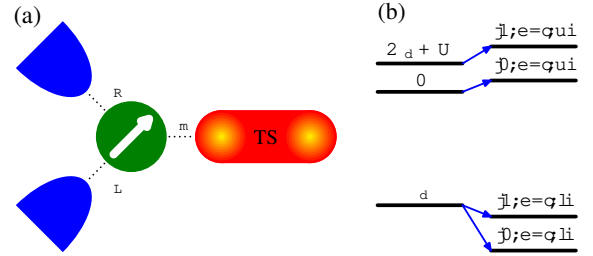


FIG. 1. (Color online) (a) Quantum dot system coupled to two normal-metal leads (by tunneling rates $\Gamma_{L(R)}$) and to one end of a floating topological superconductor (by QD-MFS tunneling rate Γ_m). We assume that only the spin- \downarrow component is coupled to the MFS. (b) Energy diagram for the (isolated) QD-MFS system showing the induced Zeeman field in the dot by the MFS.

ing in a sense that it is capacitively connected to a gate and no dc current flows through it. The two normal leads are to serve as probe of the interplay between the Kondo and Majorana physics. In our study not only the deep Kondo regime (previously addressed by an effective noninteracting theory with limited validity [42]) but also the intermediate regimes where Kondo and Majorana physics are comparable are thoroughly examined. Our findings indicate that the Kondo physics is dramatically altered depending on the relative strength of (i) the overlap of Majorana fermions states (MFS) (ϵ_m), (ii) the dot-MFS coupling (Γ_m), and (iii) the Kondo temperature (T_K). In the ideal Majorana condition ($\epsilon_m = 0$) the half-fermionic anti-Fano resonance due to the MFS reduces the Kondo value of the linear conductance by exactly a factor 3/4 in the Kondo-dominant regime ($\Gamma_m < T_K$). In the Majorana-fermion dominant phase ($\Gamma_m > T_K$), on the other hand, the spin-split Kondo resonance takes place due to the MFS-induced Zeeman splitting, which is a genuine many-body effect of the strong Coulomb interaction and the topological superconductivity.

tivity. We find that once the MFSs are strongly hybridized ($\epsilon_m > \Gamma_m$) the Kondo effect is unaffected by the MFS as demonstrated below.

Model.— Our system is mapped onto a modified two-fold degenerate Anderson model where the QD state is coupled to two normal-metal contacts and a topological superconducting wire that hosts a pair of MFSs at its ends (see Fig. 1). Due to the helical property of such end-states only one of the dot spin orientations (say spin- \downarrow) hybridizes with the fully spin-polarized nearest MFS [38, 43]. The Hamiltonian then reads

$$\mathcal{H} = \sum_{\ell\mathbf{k}\mu} \epsilon_{\mathbf{k}} c_{\ell\mathbf{k}\mu}^\dagger c_{\ell\mathbf{k}\mu} + \sum_{\mu} \epsilon_d d_{\mu}^\dagger d_{\mu} + U n_{\uparrow} n_{\downarrow} + 2i\epsilon_m \gamma_1 \gamma_2 + t_m \left(d_{\downarrow}^\dagger \gamma_1 + \gamma_1 d_{\downarrow} \right) + \sum_{\ell\mathbf{k}\mu} \left(t_{\ell} d_{\mu}^\dagger c_{\ell\mathbf{k}\mu} + (h.c.) \right), \quad (1)$$

where $c_{\ell\mathbf{k}\mu}^\dagger$ creates an electron with momentum \mathbf{k} , energy $\epsilon_{\mathbf{k}}$, and spin μ in the $\ell = L, R$ reservoir. Two normal contacts share a same flat-band structure with a half bandwidth D and density of states ρ . The operator d_{μ}^\dagger creates an electron with spin μ in dot, and $n_{\mu} = d_{\mu}^\dagger d_{\mu}$ is the dot occupation for spin μ . We focus on the case of single orbital level with energy ϵ_d and strong Coulomb interaction denoted as U . The superconducting wire, assumed to be in the topological state, has two MFSs, γ_1 and γ_2 at its two ends: the MF operators follow the Clifford algebra $\{\gamma_i, \gamma_j\} = \delta_{ij}$, where $\gamma_i = \gamma_i^\dagger$. In terms of ordinary fermionic operator f , they can be written as $\gamma_1 = (f + f^\dagger)/\sqrt{2}$, and $\gamma_2 = (f - f^\dagger)/i\sqrt{2}$. In finite-length wires, the two MFSs have a finite overlap between their wavefunctions so that their coupling can lead a finite gap represented by ϵ_m . The dot electron hybridizes (i) with the conduction electrons in the contacts with a tunneling amplitude t_{ℓ} , and (ii) with the nearest MFS with a tunneling amplitude t_m . Both couplings define the two tunneling rates: $\Gamma_{\ell} = \pi \rho t_{\ell}^2$, and $\Gamma_m = \pi \rho_{\text{dot}} t_m^2$. Throughout our study, we focus on the Kondo regime, $\epsilon_d < \epsilon_F = 0 < \epsilon_d + U$ and $\Gamma \equiv \Gamma_L + \Gamma_R \ll |\epsilon_d|$, $\epsilon_d + U$ at zero temperature, where ϵ_F is the Fermi energy.

For a non-perturbative study of the many-body effect, we adopt the well-known numerical renormalization group (NRG) method [44–46]: one can refer Ref. 47 for a review. For better efficiency, we exploit the symmetries that our system has: $[Q_{\uparrow}, \mathcal{H}] = [P_{\downarrow}, \mathcal{H}] = 0$ where Q_{\uparrow} and P_{\downarrow} are charge number operator for spin- \uparrow electrons and parity operator for the sum Q_{\downarrow} of spin- \downarrow electrons and f electrons, respectively. Note that the QD-MFS hopping changes Q_{\downarrow} by even numbers only. For the analysis, we calculate the spectral densities $A_{\mu(m)} = \sum_n |\langle n | d_{\mu}^\dagger (f^\dagger) | 0 \rangle|^2 \delta(\omega - E_n + E_0)$ and $A_{zz} = \sum_n |\langle n | S_z | 0 \rangle|^2 \delta(\omega - E_n + E_0)$, where $|n\rangle$ is the many-body eigenstate with energy E_n and $|0\rangle$ is the ground state. From the spin-resolved spectral densities the transmission through the dot can be obtained, $T(\omega) = 2\pi\Gamma_L\Gamma_R/(\Gamma_L + \Gamma_R) \sum_{\mu} A_{\mu}(\omega)$, and the linear conductance is $G = (2e^2/h)T(\omega = 0)$.

Noninteracting Case ($U = 0$).— Before addressing the full system we examine simpler cases. In the noninteract-

ing case, the effect of the MFS on the transport can be handled by using the spinless model since the MFS is coupled to spin- \downarrow electrons only [41]. Therefore, $A_{\uparrow}(\omega)$, forming a resonance peak of width Γ , is not affected by the QD-MFS coupling. On the other hand, $A_{\downarrow}(\omega)$ features the destructive interference between spin- \downarrow electrons and MFS. In the on-resonant case ($\epsilon_d = 0$) and for $\epsilon_m = 0$ and small t_m , the Fano-like anti-resonance leads to a half-dip at $\omega = 0$: $\pi\Gamma A_{\downarrow}(0)$ is reduced from 1 to 1/2. The dip width is comparable with the resonance width Γ_m in $A_m(\omega)$ which is numerically found to be $\Gamma_m \approx \pi\rho_{\text{dot}}t_m^2$ with $\rho_{\text{dot}} = 1/\Gamma$. As t_m increases further ($\Gamma_m > \Gamma$), $A_{\downarrow}(\omega)$ develops two side peaks at $\omega \sim \pm\sqrt{2}t_m$ which come from the hybridization between spin- \downarrow dot electron and MFS, while $\pi\Gamma A_{\downarrow}(0) = 1/2$ is maintained due to the zero-energy MFS [41]. Similarly, $A_m(\omega)$ also exhibits three-peak structure at $\omega = 0$ and $\pm\sqrt{2}t_m$, while the height $\pi\Gamma_m A_m(0)$ increases with t_m . Consequently, the linear conductance G at zero temperature is quantized to $e^2/h + e^2/2h = 3e^2/2h$ as long as $\epsilon_m = 0$, which signals the presence of MFS in noninteracting side-coupled nanowire setups.

Isolated QD-MFS System ($t_{\ell} = 0$).— Decoupled from the leads, the QD-MFS system can be directly diagonalized even in the presence of Coulomb interaction. It finds 8 eigenstates $|q_{\uparrow}, p_{\downarrow}; \alpha\rangle$ where $q_{\uparrow} = 0, 1$ and $p_{\downarrow} = e/o$ are quantum numbers for Q_{\uparrow} and P_{\downarrow} and $\alpha = u, l$. For $\epsilon_m = 0$, the even (e) and odd (o) states are degenerate because the MFS is energyless. $|1, e/o; l\rangle$ and $|0, e/o; l\rangle$, which would be spin-degenerate $|\uparrow\rangle$ and $|\downarrow\rangle$ states at $t_m = 0$, respectively, are now split [see Fig. 1(b)] with the induced Zeeman splitting

$$\Delta_Z = \sqrt{\frac{(\delta - \epsilon_d)^2}{4} + \frac{t_m^2}{2}} - \sqrt{\frac{\epsilon_d^2}{4} + \frac{t_m^2}{2}} - \frac{\delta}{2} \quad (2)$$

with $\delta \equiv 2\epsilon_d + U$. This is a genuine combined effect of (i) coupling to the MFS and (ii) the Coulomb interaction, and it is one of our key results. Remarkably, Δ_Z , having the sign opposite to δ , vanishes at the particle-hole symmetry point ($\delta = 0$) since it is generated by dot charge fluctuations in quite analogy to the exchange field induced by ferromagnetic contacts attached to an interacting QD [17, 19]. Upon coupling to the leads, Δ_Z becomes renormalized to Δ_Z^* , which is larger than Δ_Z : we have confirmed it by applying the Haldane's scaling theory [48]. It splits the many-body resonance, resulting in profound consequences in the Kondo state, which we will show below.

$\epsilon_m = 0$ Case.— We now present our NRG results for the case that the two MFSs do not overlap. At $t_m = 0$ both of $A_{\mu}(\omega)$ features a Kondo resonance peak centered at $\omega = 0$ with a width T_K which is the Kondo temperature: $T_K = \sqrt{\frac{\Gamma U}{2}} \exp[\frac{\pi\epsilon_d(\epsilon_d+U)}{2\Gamma U}]$ [49]. For $0 < \Gamma_m < T_K$, where Kondo correlations are stronger than the QD-MFS coupling, the physics resembles that of the noninteracting case, see the left panels in Fig. 2. $A_{\uparrow}(\omega)$ is intact; the Kondo peak at $\omega = 0$ and two resonance peaks at $\omega \approx \epsilon_d$, and $\omega \approx \epsilon_d + U$ are independent of t_m . The Fano-like anti-resonance due to the

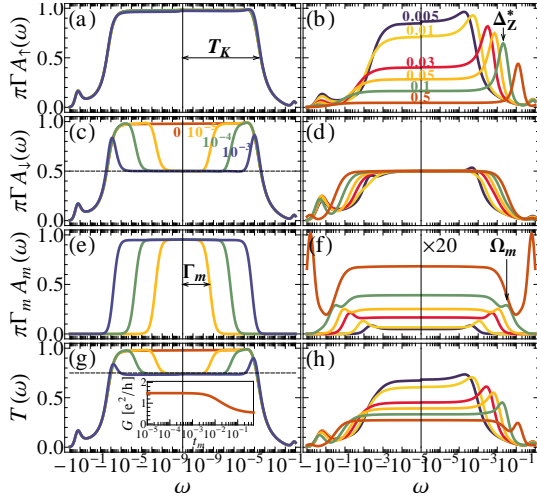


FIG. 2. (Color online) Dynamical and transport features for an ideal dot-nanowire junction with $\epsilon_m = 0$. Left and right panels represent the Kondo-dominant ($\Gamma_m < T_K$) and the MFS-dominant ($\Gamma_m > T_K$) phases, respectively: (a,b) dot spin- \uparrow spectral density, (c,d) dot spin- \downarrow spectral density, (e,f) f -operator spectral density, and (g,h) transmission coefficient for annotated values of t_m . Inset: linear conductance versus t_m . We have used $\epsilon_d = -0.2$, $U = 1$, $\Gamma_L = \Gamma_R = 0.02$, $D = 1$, and $\Gamma_m = \frac{1.2}{\Gamma} t_m^2$.

side-coupled MFS leads to a half-dip in $A_\downarrow(\omega)$, whose width is same as the width Γ_m of the Lorentzian-like resonance peak of $A_m(\omega)$. As in the noninteracting case with $\epsilon_d = 0$, the value of $A_\downarrow(\omega = 0)$ is reduced by a half: $\pi\Gamma A_\downarrow(0) = 1/2$. Therefore, the transmission coefficients $T(\omega)$ also exhibits a Kondo peak with a dip so that $T(\omega = 0) = 3/4$ and the linear conductance is pinned at $G = 3e^2/2h$. The low-energy physics in the Kondo effect can be usually understood in terms of a noninteracting model: a resonant level at $\epsilon_d^* = 0$ and with a width T_K . The observed features above might be predictable in this noninteracting frame. However, one should be very cautious in using the effective theory since t_m is found to be strongly renormalized. We numerically found that $\Gamma_m = \pi\rho_{\text{dot}}^* t_m^{*2} \approx \pi\frac{c}{\Gamma} t_m^2$ where c is a constant of order 1. Noting that $\rho_{\text{dot}}^* \sim 1/T_K$ in the Kondo regime, the renormalization should lead to $t_m^* \sim \sqrt{T_K/\Gamma} t_m$ for $\Gamma_m < T_K$. The many-body correlations are found not only to produce the

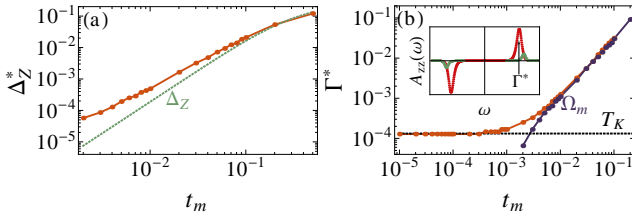


FIG. 3. (Color online) (a) Δ_Z^* and Δ_Z^* (in the MFS-dominant regime) and (b) Γ^* and Ω_m as functions of t_m . Inset: typical shape of $A_{zz}(\omega)$. We have used the same values as used in Fig. 2.

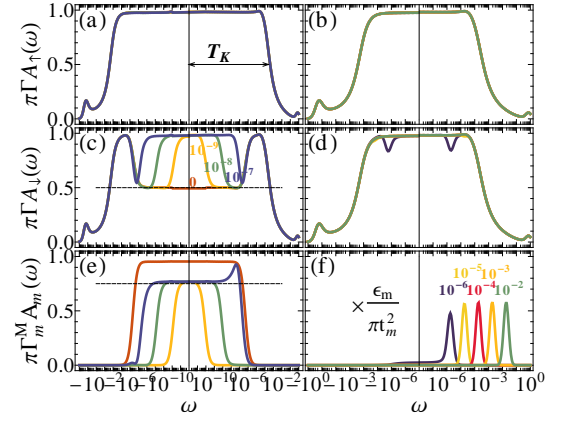


FIG. 4. (Color online). Dynamical features for a realistic wire with $\epsilon_m \neq 0$ in the Kondo dominant regime ($t_m = 10^{-4}$, $\Gamma_m < T_K$). Left and right panels represent the $\epsilon_m < \Gamma_m$ and $\epsilon_m > \Gamma_m$ cases, respectively: (a,b) dot spin- \uparrow spectral density, (c,d) dot spin- \downarrow spectral density, (e,f) f -operator spectral density for annotated values of ϵ_m . We have used the same values as used in Fig. 2 for other parameters.

Kondo effect but also to affect the QD-MFS coupling strongly.

For $\Gamma_m > T_K$, where the QD-MFS coupling is dominant over the Kondo effect, some peculiar features different from those in the noninteracting case arise. Most interestingly, the peak of $A_\uparrow(\omega)$ shifts and get wider with increasing t_m : it moves toward positive (negative) frequencies in the electron (hole)-dominant regime, $\delta > 0$ ($\delta < 0$). Remarkably, in the particle-hole symmetry point, the Kondo peak in $A_\uparrow(\omega)$ remains at $\omega = 0$ and only gets broader. This observation is well consistent with the induced Zeeman splitting previously discussed. The peak position is then identified as the renormalized Zeeman splitting Δ_Z^* . We observed a strong renormalization of Δ_Z for smaller t_m , see Fig. 3(a): numerically we found $\Delta_Z^* \approx 0.55 t_m^{1.5}$ for $\epsilon_d = -0.2$; the constant factor and exponent depend on the system details. The central peak in $A_\downarrow(\omega)$ remains at $\omega = 0$ but gets wider with t_m , while $\pi\Gamma A_\downarrow(\omega = 0)$ is fixed to $1/2$. Its width is in par with that of the central peak in $A_m(\omega)$, reflecting the coupling between them. Note that the side-peak structure in $A_\downarrow(\omega)$ observed in the noninteracting case is missing here. Because of the shift of $A_\uparrow(\omega)$, the transmission coefficients $T(\omega)$ also moves its peak with t_m , and accordingly its value at $\omega = 0$ decreases. The linear conductance then decreases with t_m for $\Gamma_m > T_K$. However, it saturates at larger values of t_m since $A_\downarrow(\omega = 0)$ remains unchanged. In the particle-hole symmetric case ($\Delta_Z^* = 0$), A_\uparrow does not move with t_m so that the linear conductance is quite independent of t_m and $T(\omega)$ is fixed to $3/4$ for wide range of frequencies centered at $\omega = 0$.

The spectral density $A_{zz}(\omega)$ of the spin susceptibility shows other evidence of the impact of the MFS on the spin correlation. It has peaks at $\omega = \pm\Gamma^*$ when the spin fluctuations are enhanced by breaking the spin correlations, see Fig. 3(b). Hence, Γ^* should be related to the spin binding energy. We found that $\Gamma^* = T_K$ in the Kondo dominant regime ($\Gamma_m < T_K$), reflecting the Kondo correlation. In the MFS

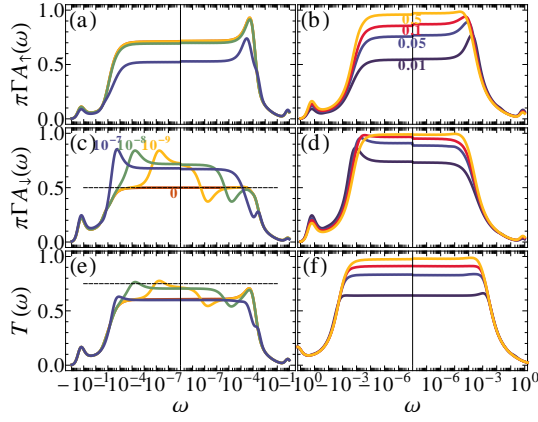


FIG. 5. (Color online). Dynamical and transport features for $\epsilon_m \neq 0$ in the MFS dominant regime ($t_m = 10^{-2}$, $\Gamma_m > T_K$) and for annotated values of ϵ_m . Left and right panels represent the $\epsilon_m < \Gamma_m$ and $\epsilon_m > \Gamma_m$ cases, respectively.

dominant regime ($\Gamma_m > T_K$) we found $\Gamma^* \approx \Omega_m$, the side peak position of $A_m(\omega)$ [see Fig. 2(f)]. In the latter case, the spin- \downarrow is more strongly hybridized with the MFS so that its correlation energy Ω_m defines the relevant spin binding energy. Note that Γ^* is not directly related to Δ_Z^* which looks more relevant to the spin correlation. We found numerically the asymptotic relation, $\Gamma^* \propto |t_m|^{1.45 \pm 0.1}$ for several values of ϵ_d in which the exponent is rather universal.

$\epsilon_m \neq 0$ Case. — In real experiments the finite size of the wire makes the two MFSs overlap, *always* giving rise to a finite $\epsilon_m \neq 0$ or the energy splitting between two fermionic levels $|0\rangle$ and $|1\rangle \equiv f^\dagger |0\rangle$. For sufficiently large splitting, $|\epsilon_m| \gtrsim \Gamma_m$, the fermionic levels at $\pm\epsilon_m$ does not interfere with the Kondo resonant level formed at the Fermi level any longer so that the Kondo physics is completely restored; see the right panels of Figs. 4 and 5. Since the lower one (say $|0\rangle$ if $\epsilon_m > 0$) is fully occupied, only the one-way transition from $|0\rangle$ to $|1\rangle$ is possible with respect to the f -fermion addition, resulting in a single-peak structure of A_m at $\omega = 2\epsilon_m$ [see Fig. 4(f)].

For smaller overlap ($\epsilon_m < \Gamma_m$) A_m is found to retain its Lorentzian-like peak at $\omega = 0$ while its width shrinks abruptly from Γ_m to $\Gamma_m^M(\epsilon_m) \approx \pi\Gamma \frac{\epsilon_m^2}{t_m^2} \approx \frac{\epsilon_m^2}{\Gamma_m}$ as soon as ϵ_m becomes finite. It is the combined effect of strong Coulomb interaction and the interference between two energy-split levels $|0/1\rangle$. The splitting of f levels accordingly affects the dot spectral densities. In the Kondo dominant regime [see Fig. 4(a,c,e)], while A_\uparrow is not so affected, A_\downarrow displays a three peak structure with a central peak of a width $\sim \Gamma_m^M$. The peak signals the disappearance of the anti-Fano resonance by the MFS at the Fermi level. It is definitely ascribed to the shift of the MFSs into finite energies ($\pm\epsilon_m$). As ϵ_m grows up to values close to Γ_m the three peaks coalesce into a single resonance, restoring the Kondo physics. The linear conductance would then show an abrupt increase from $3e^2/2h$ to $2e^2/h$ with ϵ_m , which should be smoothed at finite temperatures.

In the MFS dominant regime [see Fig. 5] the finite ϵ_m abolishes the half-fermionic Fano resonance at the Fermi level as wells: $\pi\Gamma A_\downarrow(\omega = 0)$ is not pinned to $1/2$ but larger than $1/2$ for any finite value of ϵ_m . More precisely, the half-value pinning is retained only in the finite frequencies $\Gamma_m^M < |\omega| < \Gamma_m$ for $\epsilon_m < \Gamma_m$ [see Fig. 5(c)]. Instead, the level splitting due to the finite ϵ_m produces a peak and a small dip in the opposite sides. The peak formed at $\omega \approx \mp\Gamma_m/\pi$ for $\delta \geq 0$ moves toward the higher frequencies with increasing ϵ_m until $\epsilon_m \sim \Gamma_m$ and returns to $\omega = 0$ as the Kondo physics is revived. The effective Zeeman splitting observed in A_\uparrow also diminishes with increasing ϵ_m : the peak position gradually moves toward $\omega = 0$. Hence, in contrast to the Kondo dominant case, the restoration of the linear conductance to the Kondo value is rather slow so that the full recovery is obtained for $\epsilon_m \gg \Gamma_m$ [see Fig. 5(f)].

Conclusions. — We have investigated the effect of the MFS on the Kondo physics in the side-coupled geometry. Even though the MFS is based on the superconductivity which would suppress the Kondo effect, it is found that the Kondo effect survives the interaction with the MFS in a modified form. We found that coupling to the MFS introduces an electronic way to control the effective Zeeman splitting. In addition, our results show that the energy-resolved transmission through the dot provides an excellent way to examine the properties of MFS and the overlap between the MFSs.

Acknowledgments. We acknowledge P. Simon and S. Andergassen for a critical reading of the manuscript. M. L. was supported by the CAC in KHU for computer resources and the NRF grant funded by the Korea MEST (No. 2011-0030790). R. L., and J.S. L. were supported by MINECO Grants No. FIS2011-2352 and CSD2007-00042 (CPAN).

-
- [1] A. Hewson, *The Kondo Problem to Heavy Fermions* (Cambridge University Press, New York, 1993).
 - [2] L. P. Kouwenhoven, T. H. Oosterkamp, M. W. S. Danoesastro, M. Eto, D. G. Austing, T. Honda, and S. Tarucha, *Science* **278**, 1788 (1997).
 - [3] D. Goldhaber-Gordon, J. Göres, M. A. Kastner, H. Shtrikman, D. Mahalu, and U. Meirav, *Phys. Rev. Lett.* **81**, 5225 (1998).
 - [4] D. Goldhaber-Gordon, H. Shtrikman, D. Mahalu, D. Abusch-Magder, U. Meirav, and M. A. Kastner, *Nature* **391**, 156 (1998).
 - [5] S. M. Cronenwett, T. H. Oosterkamp, and L. P. Kouwenhoven, *Science* **281**, 540 (1998).
 - [6] J. Schmid, J. Weis, K. Eberl, and K. von Klitzing, *Physica B: Condensed Matter* **256**, 182 (1998).
 - [7] W. G. van der Wiel, S. D. Franceschi, T. Fujisawa, J. M. Elzerman, S. Tarucha, and L. P. Kouwenhoven, *Science* **289**, 2105 (2000).
 - [8] J. Hygard, D. H. Cobden, and P. E. Lindelof, *Nature* **408**, 342 (2000).
 - [9] T. W. Odom, J.-L. Huang, C. L. Cheung, and C. M. Lieber, *Science* **290**, 1549 (2000).
 - [10] P. Jarillo-Herrero, J. Kong, H. S. J. van der Zant, C. Dekker, and L. P. Kouwenhoven, *Nature* **434**, 484 (2005).

- [11] O. Klochan, A. P. Micolich, A. R. Hamiltoni, K. Trunov, D. Reuter, and A. D. Wieck, Phys. Rev. Lett. **107**, 076805 (2011).
- [12] D. C. Ralph, A. W. W. Ludwig, J. von Delft, and R. A. Buhrman, Phys. Rev. Lett. **72**, 1064 (1994).
- [13] A. Kogan, S. Amasha, and M. A. Kastner, Science **304**, 1293 (2004).
- [14] S. De Franceschi, R. Hanson, W. G. van der Weil, J. M. Elzerman, J. J. Wijpkema, T. Fujisawa, S. Tarucha, and L. P. Kouwenhoven, Phys. Rev. Lett. **89**, 156801 (2002).
- [15] D. Sánchez and R. López, Phys. Rev. B **71**, 035315 (2005).
- [16] J. Park, A. N. Pasupathy, J. I. Goldsmith, C. Chang, Y. Yaish, J. R. Petta, M. Rinkoski, J. P. Sethna, H. D. Abruna, and P. L. McEuen, Nature **417**, 722 (2002).
- [17] M.-S. Choi, D. Sánchez, and R. López, Phys. Rev. Lett. **92**, 056601 (2004).
- [18] J. Martinek, Y. Utsumi, H. Imamura, J. Barnas, S. Maekawa, J. König, and G. Schon, Phys. Rev. Lett. **91**, 127203 (2003).
- [19] R. Žitko, J. S. Lim, R. López, J. Martinek, and P. Simon, Phys. Rev. Lett. **108**, 166605 (2012).
- [20] J. S. Lim, R. López, G. L. Giorgi, and D. Sánchez, Phys. Rev. B **83**, 155325 (2011).
- [21] R. Žitko, M. Lee, R. López, R. Aguado, and M.-S. Choi, Phys. Rev. Lett. **105**, 116803 (2010).
- [22] J. Alicea, Phys. Rev. B **81**, 125318 (2010).
- [23] M. Z. Hasan and C. L. Kane, Rev. Mod. Phys. **82**, 3045 (2010).
- [24] C. Beenakker, arXiv:1112.1950 (2012).
- [25] J. Alicea, arXiv:1202.1293 (2012).
- [26] A. Y. Kitaev, Physics-Uspekhi **44**, 131 (2001).
- [27] L. Fu and C. L. Kane, Phys. Rev. Lett. **100**, 096407 (2008).
- [28] V. Mourik, K. Zuo, S. M. Frolov, S. R. Plissard, E. P. A. M. Bakkers, and L. P. Kouwenhoven, Science **336**, 1003 (2012).
- [29] R. M. Lutchyn, J. D. Sau, and S. Das Sarma, Phys. Rev. Lett. **105**, 077001 (2010).
- [30] Y. Oreg, G. Rafael, and F. von Oppen, Phys. Rev. Lett. **105**, 177002 (2010).
- [31] J. Alicea, Phys. Rev. B **81**, 125318 (2010).
- [32] M. T. Deng, C. L. Yu, G. Y. Huang, P. Larsson, M. Caroff, and H. Q. Xu, arXiv:1204.4130 (2012).
- [33] A. Das, Y. Ronen, Y. Most, Y. Oreg, M. Heiblum, and H. Shtrikman, arXiv:1205.7073 (2012).
- [34] L. P. Rokhinson, X. Liu, and J. K. Furdyna, arXiv:1204.4212 (2012).
- [35] A. Zazunov, A. L. Yeyati, and R. Egger, Phys. Rev. B **84**, 165440 (2011).
- [36] R. Žitko, Phys. Rev. B **81**, 241414(R) (2010).
- [37] R. Žitko and P. Simon, Phys. Rev. B **84**, 195310 (2011).
- [38] K. Flensberg, Phys. Rev. B **82**, 180516 (2010).
- [39] L. Fu, Phys. Rev. Lett. **104**, 056402 (2010).
- [40] M. Leijnse and K. Flensberg, Phys. Rev. B **84**, 140501 (2011).
- [41] D. E. Liu and H. U. Baranger, Phys. Rev. B **84**, 201308 (2011).
- [42] A. Golub, I. Kuzmenko, and Y. Avishai, Phys. Rev. Lett. **107**, 176802 (2011).
- [43] D. Sticlet, C. Bena, P. Simon, Phys. Rev. Lett. **108**, 096802 (2012).
- [44] K. G. Wilson, Rev. Mod. Phys. **47**, 773 (1975).
- [45] H. R. Krishna-murthy, J. W. Wilkins, and K. G. Wilson, Phys. Rev. B **21**, 1003 (1980); *ibid.*, **21**, 1044 (1980).
- [46] W. Hofstetter, Phys. Rev. Lett. **85**, 1508 (2000).
- [47] R. Bulla, T. A. Costi, and T. Pruschke, Rev. Mod. Phys. **80**, 395 (2008).
- [48] F. D. M. Haldane, Phys. Rev. Lett. **40**, 416 (1978).
- [49] F. D. M. Haldane, J. Phys. C: Solid State Phys. **11**, 5015 (1978).